Tutorial: Velocity estimation via ray-based tomography

Ian F. Jones[*]

Abstract

Tomographic inversion forms the basis of all contemporary methods of updating velocity models for depth imaging. Over the past 10 years, ray-based tomography has evolved to support production of reasonably reliable images for data from complex environments for models with modest lateral velocity variation scale lengths. In this tutorial, the basics of ray-based tomography are described along with the concepts behind full waveform tomography.

Introduction

Tomography is a specific type of inversion process: in a more general framework, the field of inverse theory deals with the mathematics of describing an object based on measurements or observations that are associated with that object. A formal description of this process was given by Backus and Gilbert (1968) in the context of inverse theory applied to geophysical observations. For real industrial-scale problems, we never have sufficient observed data to determine a unique solution and the data we do have may be noisy and/or unreliable. Consequently, an entire branch of mathematics has evolved dealing with attempts to estimate a solution based on the 'interpretation of inaccurate, insufficient, and inconsistent data', as Jackson (1972) described it. In the case of travel time measurements made in a surface seismic experiment, we have a specific inverse problem where we are trying to determine the velocity structure of the earth.

What is tomography?

The word itself derives from the Greek from 'tomo' (for slice or cut) and 'graph' (to draw). In other words, we describe the structure of an object based on a collection of slices through it.

In the context of seismic imaging and velocity model building, we construct an estimate of the subsurface velocity distribution based on a series of measurements of travel times or amplitudes associated with seismic reflections, transmissions, and/or refractions, perhaps including some geological constraints (Hardy, 2003; Clapp et al., 2004). In data processing, we have access to information prior to migration (in the data domain) and also after completion of a migration in the migrated (image) domain. Within each of these domains, we have arrival time or depth (kinematic) information as well as amplitude and phase (dynamic) information; hence we have (at least) four basic classes of observables we could use to

solve the tomographic inverse problem. So, to simplify the procedure, we could use just travel time information (van de Made et al., 1984; Bishop et al., 1985; Sword, 1986; Guiziou, et al., 1990) or migrated depth information (Etgen, 1988; Stork, 1992; Kosloff et al., 1996; Bloor, 1998) or, more completely, we could use the measured amplitudes of the waveforms of the recorded data including the associated arrival times and phases (Worthington, 1984; Pratt et al., 1996). It should be noted that as this is still a developing field, particularly in the case of tomography using the full waveform, the terminology continues to evolve; hence we can easily get confused by different descriptions in the literature. Table 1 summarizes the options for performing tomographic inversion for velocity model building.

Tomography based on ray tracing can be formulated for reflection, transmission, and refraction. Several techniques for computing statics corrections in seismic reflection surveys make use of refraction tomography, whilst transmission tomography is used for cross-well applications where both the source and the receiver are inside the medium (within the boreholes) and also for VSP walk-away studies; hence we have access to, and can make use of, transmitted arrival information. Exploiting amplitude information in addition to arrival times can further assist ray-based tomography in estimating a reliable velocity model (e.g., Semtchenok et al., 2009). In addition to velocity estimation, tomography can be used to estimate other earth parameters, such as absorption. In this paper we will deal with velocity estimation, outlining the basic concepts underpinning tomographic inversion by describing just one of the many possible algorithmic approaches to solving the reflection travel time inversion problem.

To describe what tomography is, let's start by describing what it is not. Most geoscientists will be familiar with the process of Dix inversion, where the root mean square

* ION GX Technology EAME, 1st Floor Integra House, Vicarage Road, Egham, Surrey TW20 9JZ, UK.
E-mail: ian.jones@iongeo.com

	Data domain	Image (migrated) domain
Ray based (kinematic)	Reflection travel time tomography Cross-well transmission tomography Refraction tomography	Prestack time migration tomography Prestack depth migration tomography
Waveform based (dynamic)	Full waveform inversion (also known as waveform tomography, wave equation tomography, and diffraction tomography)	Wave-equation migration velocity analysis (WEM-VA) Wavepath tomography

Table 1 *Types and domains of tomography for velocity estimation.*

averages of the interval velocities down to the top and base of the nth layer in a sequence of flat layers can be used to estimate the interval velocity in the nth layer. This process is approximately valid for a flat-layered earth with no lateral velocity variation and small source-receiver offsets, because it makes the assumption that the usual small-angle approximations for trigonometric functions of the angle of incidence are valid (Sheriff and Geldart, 1995). However, if we now consider an earth model with dipping layers (Figure 1), we note that the travel path, say for zero-offset, is not made up of segments vertically above the reflection point, B, but rather by the raypath AB. To correctly estimate the interval velocity in the final layer, we should strip off the contributions encountered along the path AB and not along the (unrelated) vertical path BC, directly above the reflection point. Conventional Dix inversion, which strips off contributions vertically above the measurement, is inappropriate for either dipping layers or flat layers with lateral velocity variation within the cable length. For a fan of non-zero-offset rays, as in a common reflection point (CRP) gather, the problem would be even worse because at each offset the wavelet reflected from the horizon at B would belong to a slightly different migrated location if there is any velocity error.

One of the easiest tomographic methods to describe is the basic reflection travel time tomography problem. This deals only with the arrival times of the seismic wavelets in the input gathers for given source and receiver locations, and takes no account of the amplitude and phase of the data. Hence it falls into the category of the 'high-frequency approximation', i.e., we assume that the propagating wavelet is a spike. A related problem can be solved in the prestack migration domain, where we measure the migrated time or depth positions of the reflectors across offsets and invert to find a model that flattens primary reflection events at the same depth (or time) across offsets in the CRP gather.

A more complete solution of the problem would be to deal with all the amplitude, phase, and arrival time information for all events, including P-wave, S-wave, reflected and refracted arrivals. This is the goal of full waveform inversion, which is also referred to in the literature as
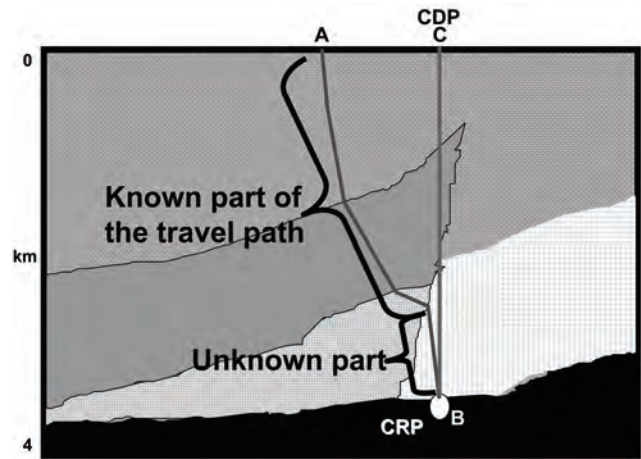

Figure 1 *Effect of dipping layers for the zero offset raypath AB.*

waveform tomography and diffraction tomography. Some implementations look at this problem for the acoustic case only (i.e., ignoring S-waves, and the effects of mode conversion on P-wave amplitudes), and some implementations also include the effects of absorption. As with the tomographic solutions in the high-frequency approximation, we can also address the full waveform inversion problem in its various forms in the migrated domain, and this is variously referred to in the literature as wave-equation migration velocity analysis (WEM-VA) or wavepath tomography (Bevc et al., 2008).

Travel time (ray) tomography

Tomography sets out to determine the interval velocity back along the individual raypaths, rather than using the false 1D assumption that the update can be purely vertical (Lines and Treitel, 1985). So, for a common midpoint (CMP) gather, tomography will try to account for the travel time observed at each offset, and use this to form an estimate of the interval velocity distribution back along each raypath in the CMP ray bundle.

In order to determine the velocity distribution, tomography tries to solve a set of simultaneous equations. Let us consider the simple 2D model in Figure 2, with the subsurface being divided into nine rectangular cells each with its own constant velocity. The arrival time for the
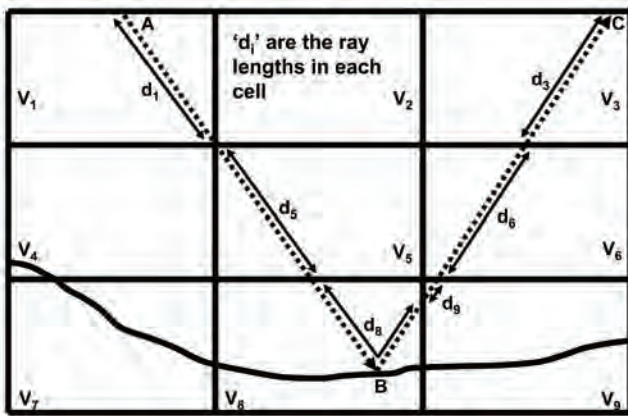
Figure 2 The earth can be described with a model comprising constant velocity cells. The total travel time for the raypath is the sum of the travel times in each cell.

Figure 3 Five raypaths corresponding to five offsets in an input gather for a nine-cell model.

raypath ABC, t_{ABC}, for a reflection event from a source at A to a receiver at C that reflects off the dipping surface at B, comprises contributions from the raypath segments in each of the cells traversed:

$$t_{ABC} = d_1/v_1 + d_5/v_5 + d_8/v_8 + d_9/v_9 + d_6/v_6 + d_3/v_3, \quad (1)$$

where d_i is the path length in the ith box with interval velocity v_i. Similar equations hold for the raypaths associated with all the offsets for this reflection event at this CMP location, and for all the CMP gathers in the survey, and for all the reflection events we can identify.

It is straightforward, in principle, to apply this same approach in 3D. If we have enough equations created in this way, we can solve for the velocity distribution in the 3D volume of cells representing our velocity model. Tomography will try to distribute the measurement errors in some equitable way throughout the 3D volume to obtain a model which best fits the observed data, i.e., the arrival times of various reflection events. Ray tracing is used within the tomography algorithm to determine the various possible raypaths and path lengths within the model cells. A more general tomographic scheme could also deal with ray bending in each cell, thus permitting vertical velocity gradients, as well as angular dependence of velocity to deal with anisotropy. Some more advanced techniques allow the cell size to vary in tandem with velocity complexity (i.e., bigger cells for smoother velocity regions, e.g., Boehm et al., 1985; Vesnaver, 1996).

To determine the velocity distribution along raypaths such as those shown in Figure 2, tomography tries to solve a set of simultaneous equations using many raypaths traversing the cells in the model. For a CMP gather, we have many travel time measurements for a given subsurface reflector element: consider the five raypaths shown in a CMP gather in Figure 3 and the associated arrival times along the moveout trajectory (Figure 4). The travel time expression for these five raypaths can be written as:
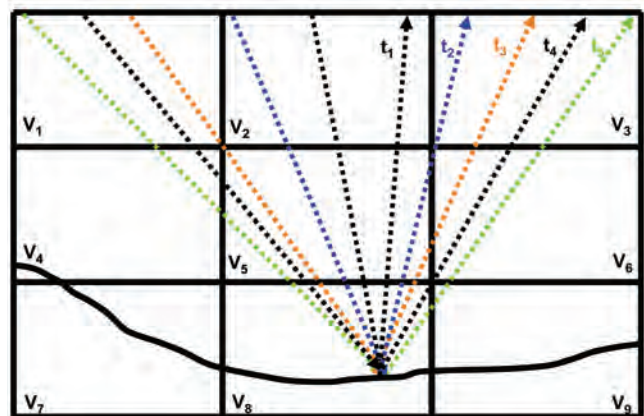
$$t_i = \sum_{j=1}^{N} d_{ij}/v_j = \sum_{j=1}^{N} d_{ij}s_j \quad (2)$$

or, in matrix notation,

$$\mathbf{T} = \mathbf{DS}, \quad (3)$$

where t_i is the total travel time along the ith raypath, d_{ij} is the length of the ith raypath in the jth cell of the velocity
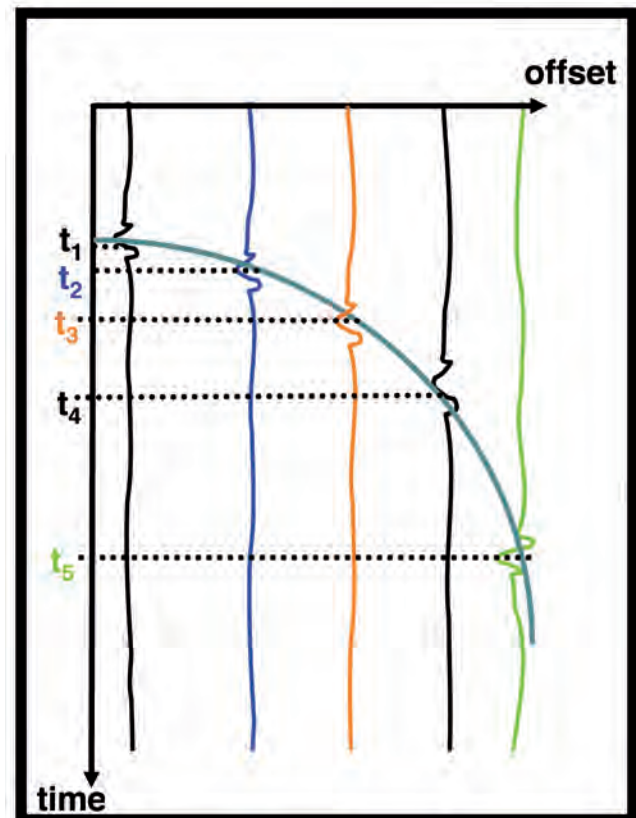

Figure 4 Moveout trajectory for a reflection event. The travel times can be measured using an autopicker.

model, v_j is the velocity in the jth cell, s_j is the slowness (i.e., the reciprocal of velocity) in the jth cell, and N is the number of cells in the model. In Figure 2, for example, $N = 9$. $\mathbf{T}$ is a column vector of M elements, the travel times for all M raypaths, and $\mathbf{S}$ is a column vector of N elements, the slowness values in each cell. $\mathbf{D}$ is a rectangular matrix of M rows and N columns whose elements are the raypath segment lengths (i.e., the values d_{ij}).

Remember that, in reality, many of the elements of the $\mathbf{D}$ matrix are zero; in other words, not all raypaths traverse all cells. We want to estimate the value of velocity in each cell of our model, so we must solve a set of simultaneous equations. We use an autopicker to measure the observed travel time for a horizon reflection event at a given offset, and we obtain estimates of the distances travelled in each cell by using a ray-tracing algorithm. Now we invert the matrix equation (3) to yield $\mathbf{S}$:

$$\mathbf{D}^{-1}\mathbf{T} = \left(\mathbf{D}^{-1}\mathbf{D}\right)\mathbf{S} = \mathbf{S}. \tag{4}$$

Unfortunately, in most cases, the matrix $\mathbf{D}$ is not invertible. To be invertible, it needs to be square (i.e., the number of travel time measurements must just happen to be the same as the number of velocity cells in the model) and also to fulfil some other criteria. So, instead, we pre-multiply both sides of equation (3) by the transpose of $\mathbf{D}$, $\mathbf{D}^{\text{T}}$, to form the symmetric square covariance matrix of $\mathbf{D}$ on the right hand side of the equation, and then seek the least squares solution of:

$$\mathbf{D}^{\text{T}}\mathbf{T} = \left(\mathbf{D}^{\text{T}}\mathbf{D}\right)\mathbf{S}. \tag{5}$$

which is

$$\mathbf{S} = \left(\mathbf{D}^{\text{T}}\mathbf{D}\right)^{-1}\mathbf{D}^{\text{T}}\mathbf{T} \tag{6}$$

There are two kinds of algorithm for solving Equation (6): a direct solver, which is a one-step solution but only suitable for smaller scale problems; and an iterative solver, such as the conjugate gradient method (Scales, 1987), which works well on large-scale systems.

However, there is a bit of a circular argument in the above description of the method: to estimate the raypath segment lengths in the cells by ray tracing, we need a velocity model and the local dip estimates of the reflector segments in each cell. But it is this velocity model that we are trying to find. Hence we start the process with forward modelling, by ray tracing using an initial guess of the model, and compute the associated travel times that we get from this first-guess model. The tomography must then iterate to try to converge on the best estimate of the true model, by minimizing the differences between the observed travel times and those computed by ray tracing for the current guess of the model.

If we also want to assess what level of detail in the model can be resolved and/or updated, we must consider all the different scale lengths involved in the picking and inversion
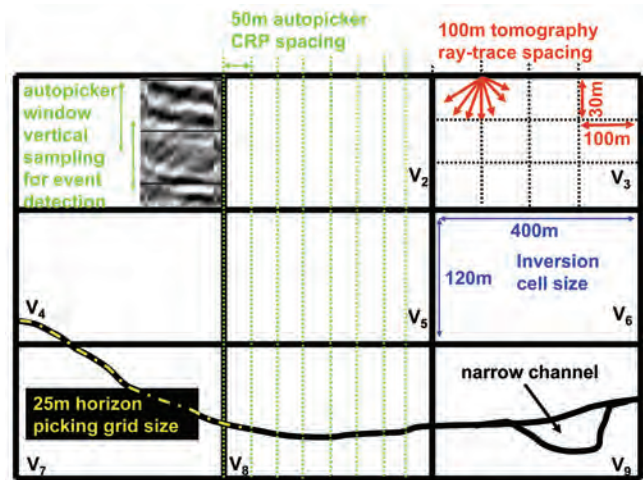

Figure 5 *Nine-cell 2D model for tomographic solution, with cell size 400 m × 120 m. Automatic picking might have been conducted with a 50 m horizontal spacing with a sliding vertical window, and the ray tracing for tomography might be performed with a 100 m horizontal spacing. Although the tomography only updates the nine macro-cells with a velocity perturbation over the entire cell, we retain the smaller features in the solution, such as the narrow channel, and the detailed interpretation of the horizon picked, say, with a 25 m horizontal spacing).*

process. The limiting factor on velocity update will be the greatest scale length used, usually the inversion grid cell size. Smaller scale features can be retained in the model if they existed in the input model (at the scale length of the velocity grid used in the tomography ray tracing, which is often the velocity sampling input to the tomography). It is important to note that the ray tracing for the forward modelling in the tomography is usually performed with a more finely sampled cell size than the one used to solve the tomographic equations. So, in effect, we are using the tomography to update only the longer spatial wavelengths of the velocity model.

We could, in principle, insert finer features into the model, say for example, by explicit picking of narrow near-surface channels. Consider, for example, an input 3D velocity field sampled at 100 m × 100 m × 30 m (in x, y and z), incorporating a 200 m wide velocity anomaly – the channel feature indicated in Figure 5. If the 3D tomography now solved for a cell size of 400 m × 400 m × 120 m, then we would still see the 200 m wide anomaly in the output velocity model, but would only have updated the longer wavelengths of the background velocity field. We can think of the process as solving the required update perturbation for the coarse 400 m × 400 m × 120 m cells, interpolating it down to the 100 m × 100 m × 30 m cells, and then adding the updated variation to the input model. The channel feature would thus persist and be retained in the updated output model.

To see how one particular type of tomographic inversion works, let us consider a gridded technique using an iterative solver (e.g., Lo and Inderwiesen, 1994) for a simple example with two rays traversing a two-cell model (Figure 6). In this case, for Equation (3) we have only the two elements in the column vector $\mathbf{T}$ for the measured arrival times t_1 and t_2. The

total distance that ray 1 travels in the first cell is d_{11}, and in the second cell is d_{12}, and so on. Hence

$$t_1 = d_{11}s_1 + d_{12}s_2 \qquad (7a)$$

$$t_2 = d_{21}s_1 + d_{22}s_2 \qquad (7b)$$

Each of these two equations can be used to represent the equation for a straight line in a 'model space' with axes s_1 and s_2 (Figure 7):

$$s_2 = t_1/d_{12} - s_1 d_{11}/d_{12} \qquad (8a)$$

$$s_2 = t_2/d_{22} - s_1 d_{21}/d_{22} \qquad (8a)$$

Anywhere along the t_1 line is a valid solution for s_1 and s_2 for that observed data measurement, but having the second travel time measurement, t_2, pins down the solution to the point of the t_1 and t_2 lines at X. If we only had the t_1 measurement, then any combination of travel path lengths could be possible between $(d_{11} = t_1/s_1, d_{12} = 0)$ and $(d_{11} = 0, d_{12} = t_1/s_2)$, as shown in Figure 7. However, our first estimates of d_{ij} are obtained by ray tracing with an initial guess of the velocity field to give starting values for the slowness in each cell, s_j, for $j = 1,2,.....N$. Therefore, our first estimates of d_{ij} are not going to be on the data lines in the model space, but at some other point, G (Figure 8):

$$t_i^{guess} = \sum_{j=1}^{N} d_{ij}^{guess} s_j^{guess} \qquad (9)$$

We need to work out a geometric solution to move point G on to, say, the t_1 line (an alternative technique would be to move G to the midpoint bisector between the t_1 and t_2 lines). We note that the small triangle denoted in the sketch with hypotenuse perpendicular to t_1 has sides Δs_1 and Δs_2. By manipulating the triangle relationships, it turns out that we can relate the changes in each s_j that we are seeking, Δs_j, to the difference between the travel time we get from ray tracing in the initial guess model and the observed travel time that has resulted from the travel path in the real earth:

$$\Delta t_i = t_i^{observed} - t_i^{guess} \qquad (10)$$

Figure 7 *With two intersecting lines, we can find the intersection representing the common solution for s_1 and s_2 at location X.*
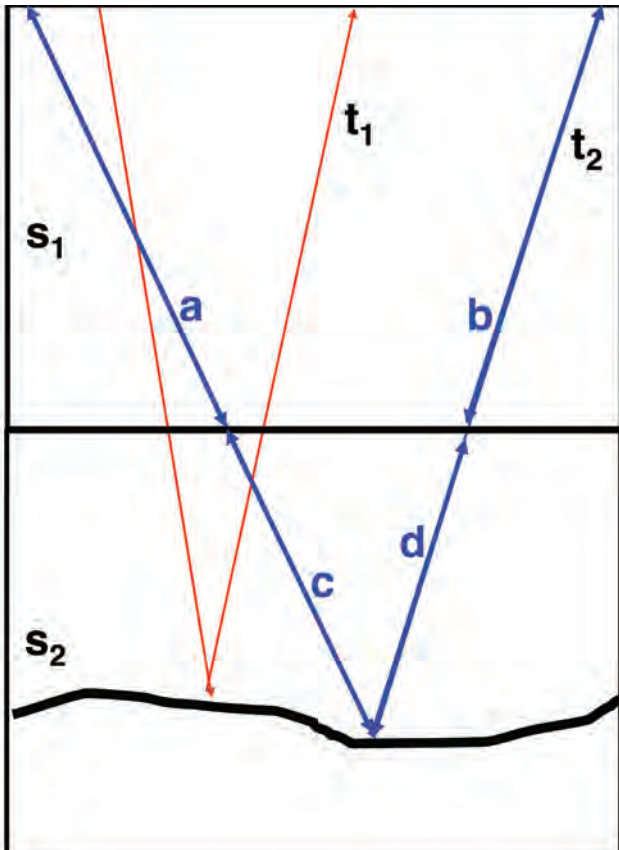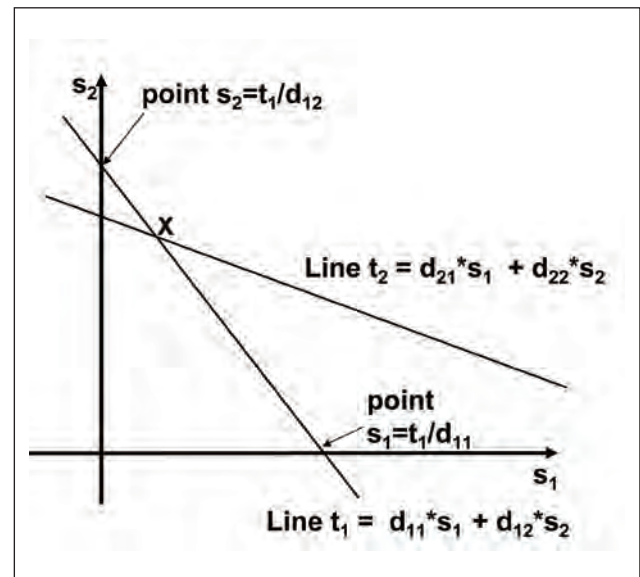

Figure 6 *Simple two-cell model with two raypaths. In this case the path lengths are made up of downgoing and upcoming segments, e.g. $d_{21}=a+b$; $d_{22}=c+d$.*
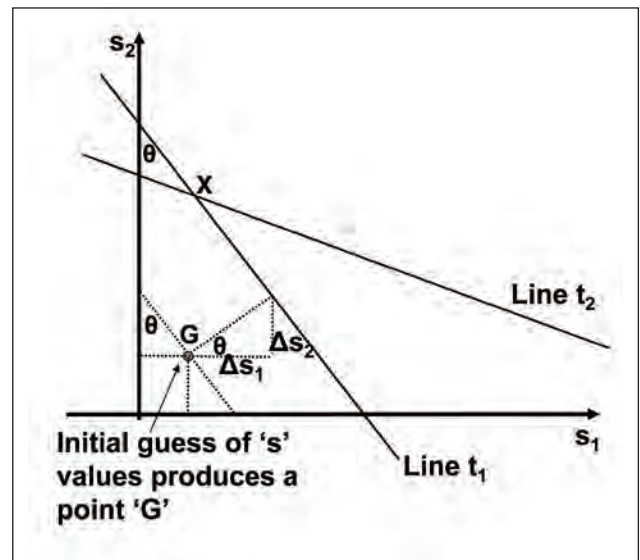

Figure 8 *Using geometrical construction, we can move from the initial point G, to an updated position on the t_1 line.*
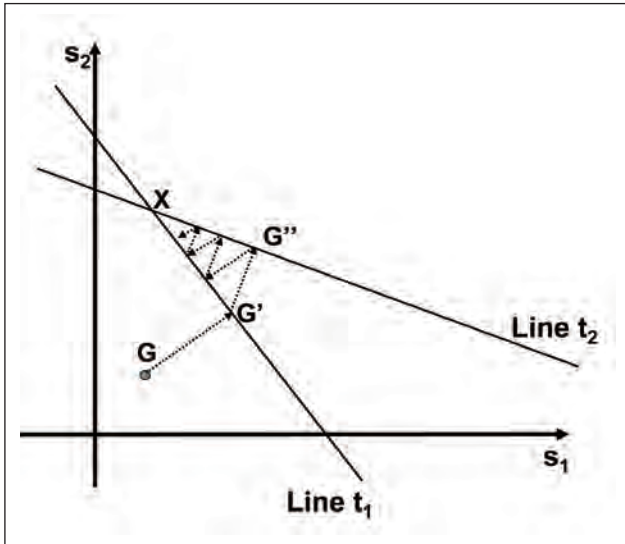
Figure 9 Iterating the model parameter estimates can converge to the vicinity of the 'correct' solution (i.e., one that adequately describes the observed data).

$$\Delta s_j = \frac{d_{ij}\Delta t_i}{\sum_{j=1}^{M}(d_{ij})^2} \tag{11}$$

Once we have moved the original guess point G to the new location on the t_1 line, at location G', we repeat the geometric exercise to find a new location G'' on the t_2 line (Figure 9). We repeat this process until we converge on location X, or at least get acceptably close to it. This is painful to work out manually, but then that is what computers are for.

Travel time (ray) tomography in the migrated domain

The procedures described so far were cast in terms of observed and ray-traced travel times from unmigrated data. Over the past decade, industrial practice has dealt primarily with data and measurements in the depth migrated domain, so we need to modify the equations being solved to account for the change of measurement domain. We also have another definition of our objective: for a given reflector element, for all acquired offsets, we must have all the modelled depths the same, i.e., primary reflection events in the CRP gathers must be flat.

Whereas in travel time tomography we trace rays iteratively following each model perturbation, here we remigrate the reflector elements iteratively. Tomography in the migrated domain can be performed after either prestack time migration (e.g., Hardy and Jeannot, 1999) or prestack depth migration (e.g., Stork, 1992), yielding a depth model in both cases, but the most widespread current industrial practice is to invert using measurements from prestack depth migrated data.

We migrate the input data with an initial guess of the velocity, and measure the depths at each offset for a given event after migration. The CRP gather in Figure 10 contains

traces from five offsets from which the residual depth errors are measured. Let the current estimate of the slowness model be s^{guess}, and the difference between the true slowness model and the guess used in the initial migration be

$$\Delta s = s^{true} - s^{guess} \tag{12}$$

We want to find the velocity model that will make the depth z of the reflector element the same across offsets in the CRP gather, so for offsets p and q, for example,

$$z_p(s^{true}) = z_q(s^{true}) \tag{13}$$

and substituting for s^{true} from Equation (12) we obtain

$$z_p(s^{guess} + \Delta s) = z_q(s^{guess} + \Delta s) \tag{14}$$

If the initial guess of the slowness model is not too far from reality, such that we can assume $\Delta s \ll s^{true}$, then we can expand the expressions for z_p and z_q as Taylor series:

$$z_p(s^{guess}) + \Delta s \frac{\partial z_p}{\partial s} = z_q(s^{guess}) + \Delta s \frac{\partial z_q}{\partial s} \tag{15}$$

The inversion process will attempt to update the slowness in all cells that influence the travel paths involved in producing the reflection at z_p. We do not have direct
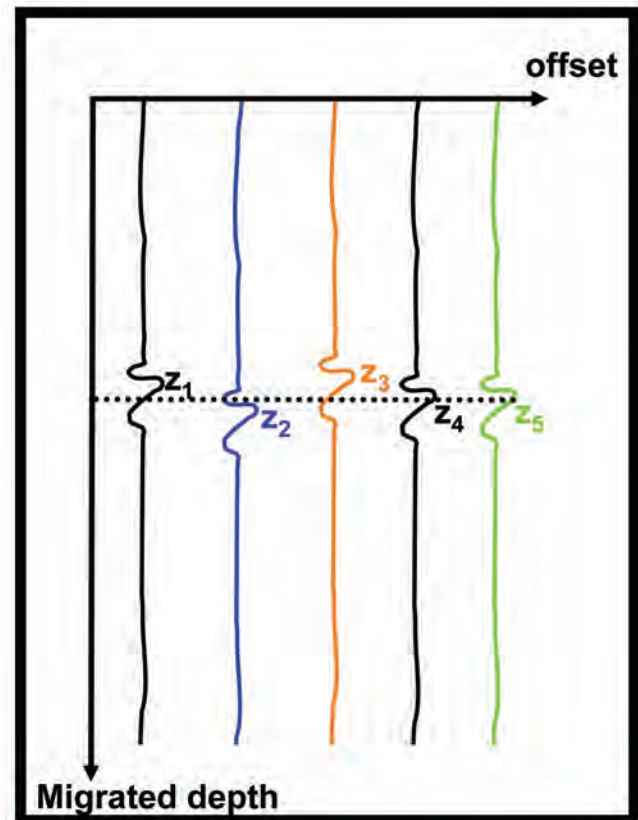

Figure 10 CRP gather showing residual depth errors.

access to the derivatives in equation (15), but we do have access to the invariant travel time information of the data. During migration, the input event at some arrival time t_p was mapped to the output location at depth z_p using the current guess of the velocity model. In the inversion scheme, we can juggle the values of depth and slowness provided that we preserve the underlying travel time t_p (Pierre Hardy, pers. comm.). We can use the chain rule of differentiation to replace the derivatives in Equation (15) as follows:

$$z_p\left(s^{\text{guess}}\right)+\Delta s \; \frac{\partial z_p}{\partial t_p}\frac{\partial t_p}{\partial s} = z_q\left(s^{\text{guess}}\right)+\Delta s \; \frac{\partial z_q}{\partial t_q}\frac{\partial t_q}{\partial s} \qquad (16)$$

and then rearrange to solve for Δs. The partial derivatives, $\partial z_p/\partial t_p$ and $\partial t_p/\partial s$, can be estimated from measurements of reflector slopes on the current iteration of migration for each offset (p, q, etc.), using the local value of s in the cell where the reflection occurs (Stork, 1992; Kosloff et al., 1996).

Resolution scale length

Velocity variation can be classified on the basis of the scale length of the variation in comparison to the wavelength of the seismic wavelet. If the velocity scale length is much greater than the seismic wavelength, then ray-based tomography using only travel time information can resolve the features. If not, then this high-frequency ray-based approach is inappropriate because diffraction behaviour will predominate, and waveform tomography (also referred to as full waveform inversion, or diffraction tomography) which uses the wavelet amplitude information must be used instead.

Figure 11 shows a situation where there is a velocity anomaly whose physical dimensions are much larger than the seismic wavelength. In this case, describing the propagating wave-front with representative rays normal to the wave-front is acceptable, because Snell's law adequately describes the refractive and reflective behaviour at the interfaces of the anomalous velocity region.

Conversely, once the velocity anomaly is of similar scale length to the seismic wavelet, as shown in Figure 12, then diffraction behaviour dominates because scattering is governing the loci of the wave-fronts. In this case, rather than just considering the arrival times of the events, we use the wave equation to estimate how the waveform will propagate through a given model, starting with some initial guess of the model. Whereas travel time tomography iterated with renditions of ray tracing, with waveform tomography we must iterate with renditions of the propagating waveform using repeated forward modelling with, for example, finite difference code, which is expensive (e.g., Pratt et al., 1996; 2002; Sirgue and Pratt, 2002; 2004).

Using the starting guess of the model, we perform a full acoustic, or elastic, finite difference modelling exercise
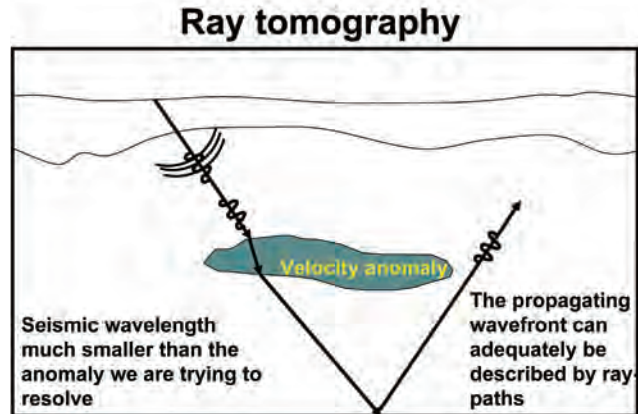

Figure 11 *Seismic wavelength much smaller than the anomaly we are trying to resolve. The propagating wavefront can adequately be described by raypaths.*
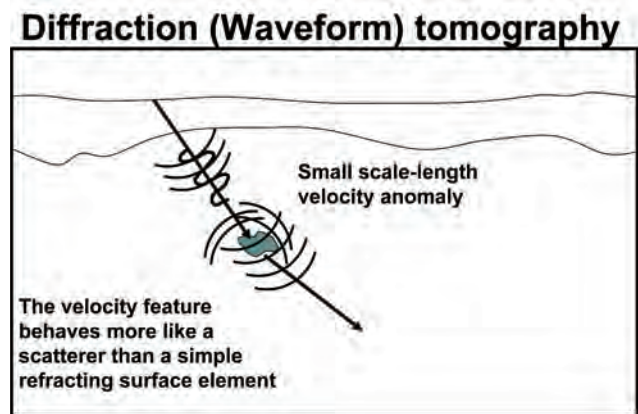

Figure 12 *Seismic wavelength larger or similar to the anomaly we are trying to resolve. The elements of the velocity feature behave more like point scatterers producing secondary wavefronts. Trying to describe the propagation behaviour as rays which obey Snell's law is no longer appropriate.*

for limited bandwidth to make a synthetic version of our recorded shot data. The real and synthetic modelled data are subtracted, and the tomography iterates to update the gridded velocity model so as to minimize this difference. In principle, this technique can resolve features smaller than the seismic wavelengths available in the recorded data, as real phase and amplitude changes are very sensitive to slight variations in the velocity. Recall that with reflection travel time tomography, we had a version that was formulated in migrated space. Likewise for full waveform inversion, which deals with unmigrated data and inverts by forward modelling to match the data, we have various counterparts that can be formulated for migrated data (e.g., Bevc et al., 2008; Vasconcelos et al., 2008). In this case we consider changes to the migrated image resulting from changes in the velocity model.

Conclusions

Tomographic inversion encompasses a powerful family of techniques that can, in principle, deliver a velocity model of the required complexity for migration. We must ensure that the basis of the tomography, whether ray or waveform,

is paired with an appropriate migration scheme. However, cost-effective implementations of full waveform inversion are only just beginning to emerge for industrial-scale problems (e.g., Sirgue et al., 2009). The information being fed to the tomography must be correct; not, for example, contaminated with multiples in the ray-based case, or converted mode cross-talk in the waveform case. Also, the information being used must be adequately sampled so that we can resolve the detail we need in the model, and thereafter migrate it accordingly.

The mathematics involved in tomography are complex, and using a tomographic algorithm does require a significant level of skill and flair for understanding the practical ramifications of the parameter selection in terms of what effect these choices have on the velocity model we obtain. However, judicious use of these techniques has been shown to provide good control of the velocity structure of the earth which enables us to produce reasonably reliable depth images of the subsurface.

Acknowledgements

References

Backus, G. and Gilbert, F. [1968] The resolving power of gross earth data. *Geophysical Journal of the Royal Astronomical Society*, **16**, 169-205.

Bevc, D., Fliedner, M.M. and Biondi, B. [2008] Wavepath tomography for model building and hazard detection. *78th SEG Annual Meeting*, Extended Abstracts, 3098-3102.

Bishop, T.N., Bube, K.P., Cutler, R.T., Langan, R.T., Love, P.L., Resnick, J.R., Shuey, R.T., Spindler, D.A. and Wyld, H.W. [1985] Tomographic determination of velocity and depth in laterally varying media. *Geophysics*, **50**, 903-923.

Bloor, R. [1998] Tomography and depth imaging. *60th EAGE Conference & Exhibition*, Expanded Abstracts, 1-01.

Boehm, G., Cavallini, F. and Vesnaver, A.L. [1995] Getting rid of the grid. *65th SEG Annual Meeting*, Extended Abstracts, 655-658.

Clapp, R.G., Biondi, B. and Claerbout, J.F. [2004] Incorporating geologic information in reflection tomography. *Geophysics*, **69**, 533–546.

Etgen, J.T. [1988] Velocity analysis using prestack depth migration: linear theory. *58th SEG Annual Meeting*, Extended Abstracts, 909-912.

Guiziou, J.L., Compte, P., Guillame, P., Scheffers, B.C., Riepen, M. and Van der Werff, T.T. [1990] SISTRE: a time-to-depth conversion tool applied to structurally complex 3-D media. *60th SEG Annual Meeting*, Extended Abstracts, 1267-1270.

Hardy, P. and Jeannot, J.P. [1999] 3D reflection tomography in time-migrated space. *69th SEG Annual Meeting*, Extended Abstracts, 1287-1290.

Hardy, P.B. [2003] High resolution tomographic MVA with automation, *SEG/EAGE summer research workshop*, Trieste.

Jackson, D.D. [1972] Interpretation of inaccurate, insufficient, and inconsistent data. *Geophysical Journal of the Royal Astronomical Society*, **28**, 97-109.

Kosloff, D., Sherwood, J., Koren, Z., Machet, E. and Falkovitz, Y. [1996] Velocity and interface depth determination by tomography of depth migrated gathers. *Geophysics*, **61**, 1511-1523.

Lines, L.R. and Treitel, S. [1985] Inversion with a grain of salt. *Geophysics*, **50**, 99-109.

Lo, T.W. and Inderwiesen, P. [1994] *Fundamentals of Seismic Tomography*. SEG, Tulsa.

Pratt, R.G., Song, Z.-M., Williamson, P. and Warner, M. [1996] Two-dimensional velocity models from wide-angle seismic data by wavefield inversion. *Geophysical Journal International*, **124**, 323-340.

Pratt, R.G., Gao, F., Zelt, C. and Levander, A. [2002] A comparison of ray-based and waveform tomography - implications for migration. *64th EAGE Conference & Exhibition*, Expanded Abstracts, B023.

Scales, J.A. [1987] Tomographic inversion via the conjugate gradient method. *Geophysics*, **52**, 179-185.

Semtchenok, N.M., Popov, M.M. and Verdel, A.R. [2009] Gaussian beam tomography. *71st EAGE Conference & Exhibition*, Expanded Abstracts, U032.

Sheriff, R.E. and Geldart, L.P. 1995. *Exploration Seismology*. Cambridge University Press.

Sirgue, L. and Pratt, R.G. [2002] Feasibility of full waveform inversion applied to sub-basalt imaging. *64th EAGE Conference & Exhibition*, Expanded Abstracts, P177.

Sirgue, L. and Pratt, R.G. [2004] Efficient waveform inversion and imaging: a strategy for selecting temporal frequencies. *Geophysics*, **69**, 231-248.

Sirgue, L., Barkved, O.I., Van Gestel, J.P., Askim, O.J. and Kommedal, J.H. [2009] 3D waveform inversion on Valhall wide-azimuth OBC. *71st EAGE Conference & Exhibition*, Expanded Abstracts, U038.

Stinson, K.J., Chan, W.K., Crase, E., Levy, S., Reshef, M. and Roth, M. [2004] Automatic imaging: velocity veracity. *66th EAGE Conference & Exhibition*, Expanded Abstracts, C018.

Stork, C. [1992] Reflection tomography in the postmigrated domain. *Geophysics*, **57**, 680-692.

Sword, C.H., Jr. [1986] Tomographic determination of interval velocities from picked reflection seismic data. *56th SEG Annual Meeting*, Extended Abstracts, 657-660.

van de Made, P.M., van Riel, P. and Berkhout, A.J. [1984] Velocity and subsurface geometry inversion by a parameter estimation in complex inhomogeneous media. *54th SEG Annual Meeting*, Extended Abstracts, 373-376.

Vasconcelos, I. [2008] Generalized representations of perturbed fields — applications in seismic interferometry and migration. *78th SEG Annual Meeting*, Extended Abstracts, 2927-2931.

Vesnaver, A.L. [1996] Irregular grids in seismic tomography and minimum-time ray tracing. *Geophysical Journal International*, **126**, 147-165.

Worthington, M.H. [1984] An introduction to geophysical tomography. *First Break*, **2**(11), 20-26.